Forced Vibrations of Damped Cylindrical Shells Filled with Pressurized Liquid

Y. P. Lu*
David W. Taylor Naval Ship R&D Center, Annapolis, Md.

An analytical formulation is presented for the forced vibratory responses of a pressurized liquid-filled cylindrical shell having a number of mass segments adhered to it by a viscoelastic material. The mass segments are distributed discretely around the outer circumference at an arbitrary section of the shell, and the excitation is a concentrated vibratory radial force located on the surface of the shell. The end conditions of the shell are assumed simply supported. The liquid is considered as a compressible and inviscid fluid. The viscoelastic material is assumed incompressible. The interaction between the shell and the attached mass segments, and the interaction between the shell and the enclosed liquid are taken into consideration. The driving point mechanical impedances are given for a location midway between two mass segments and half the distance along the length for a given damped system with or without pressurized water. These solutions are compared and discussed, respectively, with those of an undamped shell. The response of a discontinuously constrained damped ring configuration without liquid enclosed, and the frequencies of an undamped shell filled with pressurized water, which are the special cases derived from the analysis presented, respectively, compare very well with the available experimental data. A simple method for measuring the complex dynamic moduli of damping materials also is suggested.

Nomenclature

a	= radius of middle surface of shell
b_i	= circumferential length of mass segment i
c	= wave speed of fluid
D	$= 2Eh_1/(1-\nu^2)$, extensional rigidity
d_i	= width of mass segment i
E	= Young's modulus of elasticity of shell material
E^*	= Young's modulus of elasticity of viscoelastic material
F_x, F_θ, F_r	= general concentrated loading functions
F_r^c	= concentrated loading
F_θ^i, F_r^i	= reaction forces due to mass segment i attachment
G^*	= shear modulus of the viscoelastic material
$2h_1$	= thickness of shell
$2h_2$	= thickness of viscoelastic layer
$2h_i$	= thickness of mass segment i
I_n	= nth order modified Bessel function of the first kind
J_n	= nth order Bessel function of the first kind
K_{ij}	= elements of the stiffness matrix
k	$= h_1^2/(3a^2)$
k^*	$= E^* b_i d_i/(2h_2)$, compression-tension spring constant
k_s^*	$= G^* b_i d_i/(2h_2)$, shear spring constant
ℓ	= length of shell
M	$= 2\rho h_1 a \Omega^2/D$
m	= longitudinal half-wave number
m_i	$= 2\rho_i b_i d_i h_i$, mass of mass segment i
N	= total number of attached mass segments
n	= circumferential wave number
p	= internal pressure
p_x, p_θ, p_r	= surface loadings
$p_{x0}, p_{\theta 0}, p_{r0}$	= amplitudes of concentrated loadings
t	= time variable
u, v, w	= axial, circumferential, and radial displacement components of shell
u_1, v_1, w_1	= displacement components of shell because of F_r^c
u_2, v_2, w_2	= displacement components of shell because of F_θ^i and F_r^i
v_i, w_i	= displacement components of mass segment i
v_t, w_t	= total displacement components of shell with mass segments attached
r, θ, x	= cylindrical coordinates
x_c, θ_c	= coordinates of point of application of F_r^c
x_i, θ_i	= coordinates of point of attachment of mass segment i
x_0, θ_0	= coordinates of point of application of general concentrated loads
α^2	$= \Omega^2/c^2 - \lambda^2$
β'^2	$= \lambda^2 - \Omega^2/c^2$
β	= loss factor of the viscoelastic material
ϵ_n	= Neumann factor
λ	$= m\pi/\ell$
ν	= Poisson's ratio of shell material
ρ_i	= mass density of mass segment i
ρ	= mass density of shell material
ρ_f	= mass density of fluid
Ω	= excitation frequency

Received Oct. 14, 1976; revision received June 3, 1977.
Index categories: Structural Dynamics; Structural Composite Materials.

*Senior Project Engineer.

I. Introduction

IN coping with modern problems of structural resonance caused by the complex nature of the dynamic environment and the requirement of design objectives which include low noise, light weight, long life, and increased reliability, conventional structural designs are often made unacceptable. One approach to solving the high vibration and noise levels of structural resonance problems is to incorporate high-energy-dissipating mechanisms into the structural fabrication.

It is known that noise and vibration can be reduced by the dissipation of energy within the vibrating members themselves by utilizing layers of viscoelastic shear damping material. A combination of viscoelastic damping material and metal will provide strength and rigidity but with a low response to vibration. One configuration of adoption of such technique is to induce a shear strain in the damping material by bonding it between two layers of much more rigid materials to form a sandwich[1-5] in which most of the shear deformation that occurs during flexing of the sandwich will be in the middle layer, consisting of the less rigid damping material, and energy will be dissipated in every section of this layer. Other damping arrangements include configurations such as those based on the cell-insert design concept conceived by Ruzicka,[6,7] also described as constrained viscoelastic layer systems by Ungar and Kerwin[8] such as damping tapes, spaced damped treatment, laminated structures, strip dampers, and various other configurations utilizing the same principle, i.e., to employ viscoelastic shear-damping mechanisms that produce the desired energy dissipation during flexural vibrations. The purposes of all various treatments tend to offer the possibility of effective damping over a wide range of frequencies for given engineering requirements and applications. In this paper, we suggest a configuration of a damped cylindrical shell filled with pressurized liquid along with the utilization of the shear-damping material.

In dealing with the damped system, there are generally two problem areas considered. One is the structural problem, and the other is the control problem. The former is to find the structural responses of the system when the damping material properties are given. The latter is to find the proper damping material so as to optimize the structural response for a given application or requirement when the response obtained is not what one wishes to have. An analysis of the first problem area forms the subject matter of this paper.

In recent years, analytical formulations[9,10] for the forced responses of a discontinuously constrained damped ring have been presented. The structural system considered is a damped composite ring made of a thin-walled ring having a finite number of mass segments equally spaced and uniformly attached to its circumference by a thin viscoelastic material layer. Experimental and theoretical results are compared and discussed for the radial driving point mechanical impedances of such a discontinuously constrained structure. The problem under consideration in this paper is to solve a more general case for the damped cylindrical shell system by using interaction formulation. Specifically, an analysis is presented for the forced vibratory responses of a pressurized liquid-filled cylindrical shell having a number of mass segments adhered to it externally by a viscoelastic material layer at an arbitrary section of the shell. The mass segments are distributed discretely around the circumference of the shell, and the excitation is a concentrated vibratory radial force located on the surface of the shell. The end conditions of the shell are assumed simply supported (Fig. 1). In this analysis, the mass segments may not have to be identical, nor do their distributions have to be uniform. The liquid is considered as a compressible and inviscid fluid. The interaction between the shell and the attached mass segments, and the interaction between the shell and the enclosed liquid are considered because the dynamic reactions of the attached system and the fluid interaction loading could affect significantly the motion of the shell.

In the damped structural system, the four parts considered are the elastic cylindrical shell, the enclosed pressurized liquid, the attached mass segments, and the viscoelastic layer connecting the shell and the attached mass segments. The shell is assumed to be thin so that the ratio of its thickness to the radius of its midplane is small and that it can be described by Flügge's equation.[11] The effects of the rotatory inertia and shear deformation of the shell are neglected. The enclosed fluid is assumed to satisfy the wave equation. The viscoelastic material is considered incompressible and is assumed to act as

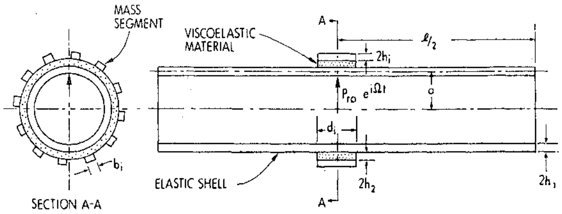

Fig. 1 Geometry of the problem.

a weightless spring between the shell and the adjacent mass segments. The effects of the operational temperature and frequency concerned on the viscoelastic material properties are taken into account. For a loading applied midway between two mass segments and half the distance along the length, the driving point mechanical impedances are presented for a given damped system in which the mass segments are attached at the middle section of the shell. These solutions are compared and discussed, respectively, with those of an undamped shell with or without the pressurized water enclosed. The response of a discontinuously constrained damped ring configuration without the presence of the liquid, and the frequencies of an undamped shell filled with pressurized water, which are the two special cases derived from the analysis presented, respectively, compare very well with the available experimental data. A simple method for measuring the complex dynamic moduli of damping materials also is suggested.

II. Mathematical Formulation

When a shell is filled with pressurized liquid and is deformed, any point of the middle surface will rotate and the resultant forces caused by the internal pressure p will be changed slightly. The components of the changed resultant forces in the r, θ, x directions for an element are[12]

$$N_x = \bar{N}_\theta \left(\frac{\partial^2 v}{\partial x \partial \theta} - \frac{\partial w}{\partial x} \right) \mathrm{d}\theta \tag{1a}$$

$$N_\theta = -\bar{N}_x \frac{\partial^2 v}{\partial x^2} \mathrm{d}x \tag{1b}$$

$$N_r = -\bar{N}_x \frac{\partial^2 w}{\partial x^2} \mathrm{d}x - \bar{N}_\theta \left[1 + \frac{1}{a} \left(\frac{\partial^2 w}{\partial \theta^2} - \frac{\partial v}{\partial \theta} \right) \right] \mathrm{d}\theta \tag{1c}$$

where the membrane forces are expressed, respectively, by $\bar{N}_x = \frac{1}{2} pa^2 \mathrm{d}\theta$ and $\bar{N}_\theta = pa\mathrm{d}x$. In Eq. (1), the terms on the right contain the rotation of the shell induced by the deformation of the displacement components. When the forces resulting from the pressurized internal loading are incorporated into the Flügge's shell equation[11] for the thin elastic circular isotropic cylindrical shell subjected to vibratory distributed pressure loadings, the linear dimensional differential equations describing the motion of its middle surface are

$$a \frac{\partial^2 u}{\partial x^2} + \frac{1-\nu}{2a} \frac{\partial^2 u}{\partial \theta^2} + \left(\frac{1+\nu}{2} - \frac{pa}{2D} \right) \frac{\partial^2 v}{\partial x \partial \theta} + \left(\nu + \frac{pa}{2D} \right) \frac{\partial w}{\partial x}$$
$$+ k \left(\frac{1-\nu}{2a} \frac{\partial^2 u}{\partial \theta^2} - a^2 \frac{\partial^3 w}{\partial x^3} + \frac{1-\nu}{2} \frac{\partial^3 w}{\partial x \partial \theta^2} \right)$$
$$+ \frac{a}{D} p_x = -\frac{2\rho h_1 a}{D} \Omega^2 u \tag{2a}$$

$$\left(\frac{1+\nu}{2} - \frac{pa}{2D} \right) \frac{\partial^2 u}{\partial x \partial \theta} + \frac{1}{a} \frac{\partial^2 v}{\partial \theta^2} + \left[\frac{a(1-\nu)}{2} + \frac{pa^2}{2D} \right] \frac{\partial^2 v}{\partial x^2}$$
$$+ \left(\frac{1}{a} + \frac{p}{2D} \right) \frac{\partial w}{\partial \theta} + k \left[\frac{3}{2} a (1-\nu) \frac{\partial^2 v}{\partial x^2} \right.$$
$$\left. - \frac{a(3-\nu)}{2} \frac{\partial^3 w}{\partial x^2 \partial \theta} \right] + \frac{a}{D} p_\theta = -\frac{2\rho h_1 a}{D} \Omega^2 v \tag{2b}$$

$$\left(\nu + \frac{pa}{2D} \right) \frac{\partial u}{\partial x} + \left(\frac{1}{a} + \frac{p}{2D} \right) \frac{\partial v}{\partial \theta} + \frac{w}{a} - \frac{pa^2}{2D} \frac{\partial^2 w}{\partial x^2}$$
$$- \frac{p}{D} \frac{\partial^2 w}{\partial \theta^2} - \frac{a}{D} p_r + k \left[\frac{1-\nu}{2} \frac{\partial^3 u}{\partial x \partial \theta^2} - a^2 \frac{\partial^3 u}{\partial x^3} \right.$$

$$-\frac{a}{2}(3-\nu)\frac{\partial^3 v}{\partial x^2\partial\theta}+a^3\frac{\partial^4 w}{\partial x^4}+2a\frac{\partial^4 w}{\partial x^2\partial\theta^2}$$

$$+\frac{\partial^4 w}{a\partial\theta^4}+2\frac{\partial^2 w}{a\partial\theta^2}+\frac{w}{a}\Bigg]=\frac{2\rho h_1 a}{D}\Omega^2 w \qquad (2c)$$

where the undeformed middle surface radius, and thickness of the shell are a and $2h_1$, respectively. The material properties of the shell are Young's modulus of elasticity E, mass density ρ, and Poisson's ratio ν. The axial, circumferential, and radial displacement components of the middle surface of the shell are denoted by u, v, and w, and the circular frequency of excitation is specified by Ω. The surface loadings are expressed by p_x, p_θ, and p_r in their respective positive directions. A dimensionless quantity k is defined by $h_1^2/(3a^2)$, and the extensional rigidity of the shell is represented by D. The shell is assumed to be initially at rest.

For simply supported end conditions, let us assume

$$u=\sum_{m=0}^{\infty}\sum_{n=0}^{\infty} u_{mn}\cos\frac{m\pi x}{\ell}\cos n\theta \qquad (3a)$$

$$v=\sum_{m=0}^{\infty}\sum_{n=0}^{\infty} v_{mn}\sin\frac{m\pi x}{\ell}\sin n\theta \qquad (3b)$$

$$w=\sum_{m=0}^{\infty}\sum_{n=0}^{\infty} w_{mn}\sin\frac{m\pi x}{\ell}\cos n\theta \qquad (3c)$$

where m and n are the longitudinal half-wave number and the circumferential wave number, respectively, and the length of the shell is denoted by ℓ. The time dependent factor $e^{i\Omega t}$ is assumed, and is omitted throughout. Substituting Eq. (3) into Eq. (2), and utilizing the orthogonality relations of the sine and cosine functions, one obtains a set of reduced linear algebraic equations of motion of the shell, for each value of m and n

$$\begin{bmatrix} K_{11}-M & K_{12} & K_{13} \\ K_{12} & K_{22}-M & K_{23} \\ K_{13} & K_{23} & K_{33}-M \end{bmatrix}\begin{bmatrix} u_{mn} \\ v_{mn} \\ w_{mn}\end{bmatrix}=\begin{bmatrix} F_x \\ F_\theta \\ F_r\end{bmatrix} \qquad (4)$$

where

$$K_{11}=a\lambda^2+\frac{1-\nu}{2a}n^2(1+k) \qquad (5a)$$

$$K_{12}=-\frac{1}{2}(1+\nu)\lambda n+\frac{pa}{2D}\lambda n \qquad (5b)$$

$$K_{13}=-\nu\lambda-a^2k\lambda^3+\frac{1}{2}(1-\nu)k\lambda n^2-\frac{pa}{2D}\lambda \qquad (5c)$$

$$K_{22}=\frac{n^2}{a}+\frac{1}{2}a(1-\nu)\lambda^2(1+3k)+\frac{pa^2}{2D}\lambda^2 \qquad (5d)$$

$$K_{23}=\frac{n}{a}+\frac{1}{2}ka(3-\nu)\lambda^2 n+\frac{pn}{2D} \qquad (5e)$$

$$K_{33}=\frac{1}{a}+a^3k\lambda^4+2ak\lambda^2n^2+\frac{k}{a}n^4$$

$$-\frac{2}{a}n^2k+\frac{k}{a}+\frac{p}{2D}(a^2\lambda^2+2n^2)-Q_n \qquad (5f)$$

$$Q_n=\frac{a}{D}\rho_f\Omega^2\frac{I_n(\beta' a)}{\beta' I_n'(\beta' a)} \quad \text{if } \beta'^2=\lambda^2-\frac{\Omega^2}{c^2}>0 \qquad (5g)$$

$$Q_n=\frac{a}{D}\rho_f\Omega^2\frac{J_n(\alpha a)}{\alpha J_n'(\alpha a)} \quad \text{if } \alpha^2=\frac{\Omega^2}{c^2}-\lambda^2>0 \qquad (5h)$$

$$M=2\rho h_1 a\Omega^2/D \qquad (5i)$$

$$\lambda=m\pi/\ell \qquad (5j)$$

$$F_x=2p_{x0}\cos\lambda x_0\cos n\theta_0/(D\ell\epsilon_n\pi) \qquad (5k)$$

$$F_\theta=2p_{\theta 0}\sin\lambda x_0\sin n\theta_0/(D\ell\pi) \qquad (5l)$$

$$F_r=2p_{r0}\sin\lambda x_0\cos n\theta_0/(D\ell\epsilon_n\pi) \qquad (5m)$$

The amplitudes of concentrated loadings in each direction are expressed, respectively, by p_{x0}, $p_{\theta 0}$, and p_{r0}, and the coordinates of the point of application are $x=x_0$, and $\theta=\theta_0$. The Neumann factor ϵ_n equals two for $n=0$, and one otherwise. For given concentrated loads to a specific problem, the axial, circumferential, and radial displacement components at arbitrary points on the middle surface of the pressurized liquid-filled shell can be solved.

It should be noted that the interaction loading because of the containing fluid appears in the quantity K_{33}. In obtaining the interacting loading p_f, the fluid is assumed to be described by the wave equation. Expressing p_f in Fourier series and introducing the condition of continuity of the normal velocity and pressure on the shell/fluid interface, as well as the condition of being finite on the shell centerline, the loading yields

$$p_{mn}=\frac{\rho_f\Omega^2 w_{mn}I_n(\beta' a)}{\beta' I_n'(\beta' a)} \qquad (6)$$

if $\beta'^2=\lambda^2-\Omega^2/c^2>0$, or

$$p_{mn}=\frac{\rho_f\Omega^2 w_{mn}J_n(\alpha a)}{\alpha J_n'(\alpha a)} \qquad (7)$$

if $\alpha^2=\Omega^2/c^2-\lambda^2>0$. In Eqs. (6) and (7), the quantities $J_n(\alpha a)$ and $I_n(\beta' a)$ are the nth order Bessel function and the modified Bessel function of the first kind, respectively, and $J_n'(\alpha a)$ and $I_n'(\beta' a)$ are their derivatives with respect to the argument. The mass density and the wave speed of the fluid are denoted respectively by ρ_f and c. It is noted further that the contained fluid is assumed nonviscous; it is unable to exert shear stress. Only the interaction loading in the radial direction is considered.

For the problem under consideration, the system includes the elastic cylindrical shell with the contained pressurized fluid, the attached mass segments, and the viscoelastic springs connecting the shell and the attached mass segments. To provide a complete solution, the following three dynamic problems first are solved: 1) the dynamic response of the pressurized fluid-filled shell to the radial concentrated loading, 2) the dynamic response of each attached mass segment to the motion input at the respective point of attachments, and 3) the dynamic response of the pressurized fluid-filled shell to the dynamic reaction forces of each attached system acting at the point of attachment. The resulting response of the total system then is obtained by combining the foregoing solutions through the application of the linear superposition principle.

Consider that the shell is excited only in the outward radial direction by a time harmonic concentrated loading and applied at the point having the coordinates $x=x_c$, and $\theta=\theta_c$. The radial and the circumferential displacement components $w_1(\theta,x)$, $v_1(\theta,x)$ at any arbitrary point on the middle surface of the shell can be determined by

$$w_1(\theta,x)=\sum_{m=0}^{\infty}\sum_{n=0}^{\infty} w_{mn}^c\sin\lambda x\cos n\theta \qquad (8a)$$

$$v_1(\theta,x)=\sum_{m=0}^{\infty}\sum_{n=0}^{\infty} v_{mn}^c\sin\lambda x\sin n\theta \qquad (8b)$$

where

$$w^c_{mn} = \frac{F^c_r}{\Delta}[(K_{11}-M)(K_{22}-M)-K^2_{12}] \tag{9a}$$

$$v^c_{mn} = -\frac{F^c_r}{\Delta}[K_{23}(K_{11}-M)-K_{12}K_{13}] \tag{9b}$$

$$F^c_r = 2p_{r0}\sin\lambda x_c \cos n\theta_c/(D\ell\epsilon_n\pi) \tag{9c}$$

The determinant of the matrix given in Eq. (4) is denoted by Δ. The axial displacement component $u_1\ (\theta,x)$ can be obtained likewise.

For each attached mass segment, it is considered to be a single degree-of-freedom system. For simplicity, the rotational motion about the center of mass of the mass segment is neglected, nor is the interaction between the segment and the shell in the longitudinal direction included. The equations of motion in the radial and circumferential directions can be written as

$$-m_i\Omega^2 w_i + k^*[w_i - w_t(\theta_i,x_i)] = 0 \tag{10a}$$

$$-m_i\Omega^2 v_i + k^*_s[v_i - v_t(\theta_i,x_i)] = 0 \tag{10b}$$

where w_i and v_i are the radial and circumferential displacement components, respectively, of the mass segment i whose mass is represented by m_i. The quantities $w_t(\theta_i,x_i)$ and $v_t(\theta_i,x_i)$, which are unknown and yet to be determined, are the total response in the radial and circumferential directions at the point of attachment of mass segment i. Note that the point of attachment is assumed to be on the middle surface instead of on the surface of the shell. This is a reasonable assumption for a thin shell. The equivalent compression-tension, and shear spring constants k^* and k^*_s depend on the geometry of the mass segment, the thickness of the viscoelastic layer, and material properties of the viscoelastic material. The viscoelastic material properties, which are complex, are assumed temperature and frequency dependent, and the strain amplitude dependence of the properties is neglected. The spring constants are

$$k^* = E^* b_i d_i/(2h_2) \tag{11a}$$

$$k^*_s = G^* b_i d_i/(2h_2) \tag{11b}$$

where the circumferential length of the mass segment i is b_i, and the width is d_i. The viscoelastic layer has Young's modulus of elasticity E^*, and shear modulus G^*, and its thickness $2h_2$. The viscoelastic material used is assumed incompressible. This assumption is approximately true for most viscoelastic materials, as verified by Cramer,[13] and, hence, there will not be any difference in the values for the loss factors in shear and in direct deformation. It is obvious that mass segments may not have to be identical, nor do their distributions have to be uniform. From Eq. (10), the relationships between w_i and $w_t(\theta_i,x_i)$, v_i and $v_t(\theta_i,x_i)$ can be written as

$$w_i = C_1 w_t(\theta_i,x_i) \tag{12a}$$

$$v_i = C_s v_t(\theta_i,x_i) \tag{12b}$$

where

$$C_1 = k^*/(k^*-m_i\Omega^2) \tag{13a}$$

$$C_s = k^*_s/(k^*_s-m_i\Omega^2) \tag{13b}$$

The dynamic reaction force due to the presence of the attached mass segment can be considered as point loadings acting at the point of attachment in the radial as well as in the circumferential directions. For the mass segment i attached at a point having the coordinates $x=x_i$ and $\theta=\theta_i$, the dynamic responses in the radial and circumferential directions $w_2(\theta,x)$ and $v_2(\theta,x)$ at any arbitrary point on the middle surface of the shell to these reaction forces give

$$w_2(\theta,x) = \sum_{m=0}^{\infty}\sum_{n=0}^{\infty} w^i_{mn}\sin\lambda x\cos n\theta \tag{14a}$$

$$v_2(\theta,x) = \sum_{m=0}^{\infty}\sum_{n=0}^{\infty} v^i_{mn}\sin\lambda x\sin n\theta \tag{14b}$$

where

$$w^i_{mn} = -\frac{F^i_\theta}{\Delta}[K_{23}(K_{11}-M)-K_{12}K_{13}] + \frac{F^i_r}{\Delta}[(K_{11}-M)(K_{22}-M)-K^2_{12}] \tag{15a}$$

$$v^i_{mn} = \frac{F^i_\theta}{\Delta}[(K_{11}-M)(K_{33}-M)-K^2_{13}] - \frac{F^i_r}{\Delta}[K_{23}(K_{11}-M)-K_{12}K_{13}] \tag{15b}$$

$$F^i_\theta = \frac{2}{D\ell\pi}k^*_s v_t(\theta_i,x_i)(C_s-1)\sin\lambda x_i\sin n\theta_i \tag{15c}$$

$$F^i_r = \frac{2}{D\ell\epsilon_n\pi}k^* w_t(\theta_i,x_i)(C_1-1)\sin\lambda x_i\cos n\theta_i \tag{15d}$$

Likewise, the axial displacement component $u_2(\theta,x)$ can be determined. In Eqs. (14) and (15), the terms containing the elasticity modulus E^* relate the energy dissipation because of extensional strain, whereas the terms with the shear modulus G^* involve the energy dissipation by shear deformation.

Having solved the preceding three subproblems, it is possible to calculate the total radial and circumferential deflections $w_t(\theta,x)$ and $v_t(\theta,x)$ resulting from the dynamic interaction as the sum of the shell response to the radial concentrated loading and the dynamic reaction forces of the attached mass segments based on the linear superposition principle. Combining Eqs. (8, 10, and 14), the total radial and circumferential displacement components give

$$w_t(\theta,x) = \sum_{m=0}^{\infty}\sum_{n=0}^{\infty}\frac{F^c_r}{\Delta}[(K_{11}-M)(K_{22}-M)-K^2_{12}] \times\sin\lambda x\cos n\theta + \sum_{i=1}^{N}\sum_{m=0}^{\infty}\sum_{n=0}^{\infty}\frac{F^i_r}{\Delta}[(K_{11}-M)(K_{22}-M) - K^2_{12}]\sin\lambda x\cos n\theta - \sum_{i=1}^{N}\sum_{m=0}^{\infty}\sum_{n=0}^{\infty}\frac{F^i_\theta}{\Delta}[K_{23} \times(K_{11}-M)-K_{12}K_{13}]\sin\lambda x\cos n\theta \tag{16a}$$

$$v_t(\theta,x) = -\sum_{m=0}^{\infty}\sum_{n=0}^{\infty}\frac{F^c_r}{\Delta}[K_{23}(K_{11}-M)-K_{12}K_{13}]\sin\lambda x\sin n\theta - \sum_{i=1}^{N}\sum_{m=0}^{\infty}\sum_{n=0}^{\infty}\frac{F^i_r}{\Delta}[K_{23}(K_{11}-M)-K_{12}K_{13}]\sin\lambda x\sin n\theta + \sum_{i=1}^{N}\sum_{m=0}^{\infty}\sum_{n=0}^{\infty}\frac{F^i_\theta}{\Delta}[(K_{11}-M)(K_{33}-M)-K^2_{13}]\sin\lambda x\sin n\theta \tag{16b}$$

The first term is the response caused by the radial concentrated load applied at (θ_c,x_c), and the other two terms are the responses caused by the reaction forces of the attached mass segments. The number of mass segments is represented by N. Note that the displacement components given in Eq. (16) are coupled with each other. To find the response at any arbitrary location, the unknown total displacement components at all points of attachments $v_t(\theta_i,x_i)$ and $w_t(\theta_i,x_i)$ first must be solved by using Eq. (16) which is a set of $2N$ simultaneous linear algebraic equations with complex coefficients. Should the symmetric property exist in the mass segments attachment distribution, the size of the simultaneous equations obviously can be reduced. Once the displacement components are found, their mechanical impedances can be determined.

Since one of the primary objectives of employing the damped composite structure is to attenuate the vibratory response at the resonant conditions, to find the resonance frequency of such a system is of great importance. However, the usual procedure used in vibration analysis to find the frequencies hardly can be followed for such a composite system because the characteristic equation for each mode is difficult to obtain. In addition, because of the linear superposition application and the nature of the frequency-dependent material properties, it is a formidable task to obtain the resonance frequency for such a damped system. It is believed that using the forced vibration analysis given in this section is probably the most straightforward procedure to determine the resonance frequencies. The frequencies can be located when the slopes of responses between two frequencies change signs in the neighborhood of resonant conditions.

III. Experimental Verification of Reduced Special Cases

The analysis presented in the previous section gives a detailed formulation of the forced responses of damped cylindrical shells filled with pressurized liquid. To date, there are no experimental data available to be used to evaluate the validity and adequacy of the analytical consideration of such a problem. However, test results for special cases reduced from the problem of interest are available, and the comparison between the experimental results and the theoretical solutions of these special cases can be offered to serve as a means for verifying the analysis and the method of computation. One of the special cases which can be derived from the considered problem is to reduce it to the problem of vibrations of a discontinuously constrained damped ring configuration without the presence of liquid, and the other is to reduce it to the problem of vibrations of an undamped shell with the pressurized liquid enclosed.

Vibrations of Discontinuously Constrained Damped Rings

For this reduced case, the damped composite ring is made of a thin-walled ring having a finite number of mass segments attached to its circumference by a viscoelastic material, and is subjected to a concentrated radial load (Fig. 2). In obtaining

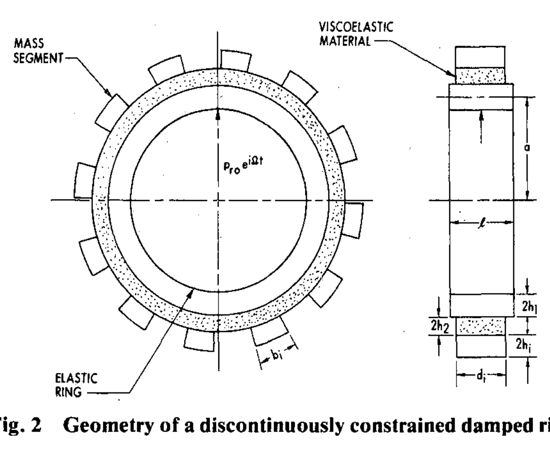

Fig. 2 Geometry of a discontinuously constrained damped ring.

the analysis derived from that given in the previous section for such a system, the differentiations of all of the physical quantities of the shell with respect to the longitudinal coordinate x, the longitudinal displacement component u, longitudinal half-wave number m, Poisson's ratio ν, and boundary conditions are suppressed. In addition, the effects caused by the pressurized fluid are neglected. Equation (8) then becomes

$$w_1(\theta) = \sum_{n=0}^{\infty} w_n^c \cos n\theta \tag{17a}$$

$$v_1(\theta) = \sum_{n=0}^{\infty} v_n^c \sin n\theta \tag{17b}$$

where

$$w_n^c = (F_r^c/\Delta)(K_{22}-M) \tag{18a}$$

$$v_n^c = -(F_r^c/\Delta)K_{23} \tag{18b}$$

$$\Delta = (K_{22}-M)(K_{33}-M) - K_{23}^2 \tag{18c}$$

$$F_r^c = p_{ro}\cos n\theta_c / (D\ell\epsilon_n\pi) \tag{18d}$$

Similarly, Eq. (14) gives

$$w_2(\theta) = \sum_{n=0}^{\infty} w_n^i \cos n\theta \tag{19a}$$

$$v_2(\theta) = \sum_{n=0}^{\infty} v_n^i \sin n\theta \tag{19b}$$

where

$$w_n^i = \frac{F_r^i}{\Delta}(K_{22}-M) - \frac{F_\theta^i}{\Delta}K_{23} \tag{20a}$$

$$v_n^i = \frac{F_\theta^i}{\Delta}(K_{33}-M) - \frac{F_r^i}{\Delta}K_{23} \tag{20b}$$

$$F_\theta^i = k_s^* v_t(\theta_i)(C_s - 1)\sin n\theta_i / (D\ell\pi) \tag{20c}$$

$$F_r^i = k^* w_t(\theta_i)(C_l - 1)\cos n\theta_i / (D\ell\epsilon_n\pi) \tag{20d}$$

In Eqs. (18) and (20), the quantities K_{22}, K_{23}, and K_{33} are the same as those given in Eq. (5) except that terms involving λ, ρ_f, and p vanish. The symbol ℓ is now the length of the ring. Since no longitudinal interaction between the mass segments and the shell is included in the formulation, Eqs. (10-13) remain unchanged for the reduced ring problem. Again, based on the linear principle of superposition, Eq. (16) is reduced to

$$w_t(\theta) = \sum_{n=0}^{\infty} \frac{F_r^c}{\Delta}(K_{22}-M)\cos n\theta + \sum_{i=1}^{N}\sum_{n=0}^{\infty} \frac{F_r^i}{\Delta}(K_{22}-M) \times \cos n\theta - \sum_{i=1}^{N}\sum_{n=0}^{\infty} \frac{F_\theta^i}{\Delta}K_{23}\cos n\theta \tag{21a}$$

$$v_t(\theta) = -\sum_{n=0}^{\infty} \frac{F_r^c}{\Delta}K_{23}\sin n\theta - \sum_{i=1}^{N}\sum_{n=0}^{\infty} \frac{F_r^i}{\Delta}K_{23}\sin n\theta + \sum_{i=1}^{N}\sum_{n=0}^{\infty} \frac{F_\theta^i}{\Delta}(K_{33}-M)\sin n\theta \tag{21b}$$

Equations (17-21) are the same as those presented for the reduced systems in Ref. 10.

The driving point mechanical impedances of a discontinuously constrained damped ring are presented in Fig. 3

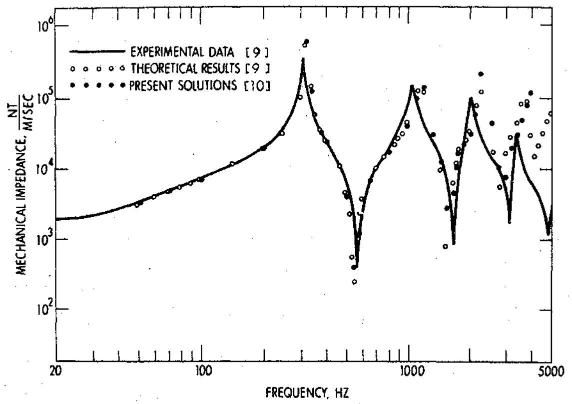

Fig. 3 Comparison of analytical and experimental results of a discontinuously constrained damped ring.

which is reproduced from an earlier paper.[10] Specifically, the system is a steel elastic ring ($a=10.3$ cm, $2h_1=1.27$ cm, $\ell=7.62$ cm) having 12 identical steel mass segments ($d_i=7.62$ cm, $2h_i=1.27$ cm, $b_i=5.08$ cm) equally spaced and uniformly attached to its circumference by an acrylic base viscoelastic material ($2h_2=1.02\times10^{-2}$ cm, at 24° C) and is subjected to a concentrated radial load. It is shown clearly that the solutions of this special case compare very well with the experimental and analytical results available.

It is interesting to note that, if only one mass segment is attached, the equation for the radial displacement component reduces to

$$w_t(\theta)=\sum_{n=0}^{\infty}\frac{F_r^c}{\Delta}(K_{22}-M)\cos n\theta+\sum_{n=0}^{\infty}\frac{F_r^i}{\Delta}(K_{22}-M)\cos n\theta \tag{22}$$

Suppose the point of application of the concentrated loading and the point of attachment of the mass segment are both at the same point, e.g., $\theta=\theta_c=0$. Equation (22) is reduced further to

$$w_t(\theta=0)=\frac{\sum_{n=0}^{\infty}\frac{p_{ro}}{D\ell\epsilon_n\pi}\frac{1}{\Delta}(K_{22}-M)}{1-\sum_{n=0}^{\infty}\frac{k^*}{D\ell\epsilon_n\pi}(C_1-1)\frac{1}{\Delta}(K_{22}-M)} \tag{23}$$

In examining the foregoing expression, it may be noted that Eq. (23) is rather simple in form and can be used to measure the complex dynamic moduli of damping materials if the experimentally measured responses and the associated phase angles at the point of attachment are available for a given system in the frequency range of interest. Rearranging Eq. (23), the dynamic moduli of the damping material can be obtained in terms of the measured response amplitude $|w_t|$ and the phase angle ϕ for a given frequency, i.e.,

$$G^*=G(1+i\beta)$$

where

$$G=\frac{1}{3}\left(\frac{y_1y_3+y_2y_4}{y_1^2+y_2^2}\right) \tag{24a}$$

$$\beta=\frac{3Gy_1-y_3}{3Gy_2} \tag{24b}$$

$$y_3=2h_2m_i\Omega^2\left[|w_t|\cos\phi-\sum_{n=0}^{\infty}\frac{p_{ro}}{D\ell\epsilon_n\pi}\frac{1}{\Delta}(K_{22}-M)\right] \tag{24c}$$

$$y_4=2h_2m_i\Omega^2|w_t|\sin\phi \tag{24d}$$

$$y_1=|w_t|\cos\phi b_i\left[d_i-m_i\Omega^2\sum_{n=0}^{\infty}\frac{K_{22}-M}{D\epsilon_n\pi\Delta}\right]-b_id_i\sum_{n=0}^{\infty}\frac{p_{ro}}{D\ell\epsilon_n\pi}\frac{1}{\Delta}(K_{22}-M) \tag{24e}$$

$$y_2=b_i|w_t|\sin\phi\left[d_i-m_i\Omega^2\sum_{n=0}^{\infty}\frac{K_{22}-M}{D\epsilon_n\pi\Delta}\right] \tag{24f}$$

Although the proposed method to measure the complex dynamic moduli of damping materials requires further studies on the reliable range over which the damping material properties are readily obtainable, the facts are that, not only is it as simple as those well-established vibrating beam techniques used for years, such as those given by Nashif,[14] Jones,[15] and Roscoe et al.,[16] but also the excellent correlation between experimental and theoretical results for a discontinuously constrained damped ring presented in Fig. 3 demonstrates that the proposed method is theoretically feasible.

Vibrations of Undamped Shell with the Pressurized Liquid Enclosed

The analysis for this special case obviously can be derived by neglecting all the effects caused by the presence of the viscoelastic layer and the attached mass segments. In obtaining the frequencies of such a system, the characteristic equation can be obtained from Eq. (4), by letting the determinant be zero, i.e.,

$$\det\begin{vmatrix}K_{11}-M & K_{12} & K_{13}\\ K_{12} & K_{22}-M & K_{23}\\ K_{13} & K_{23} & K_{33}-M\end{vmatrix}=0 \tag{25}$$

For given values of m and n, the resonant frequencies can be determined numerically because this frequency equation is transcendental.

Presented in Table 1 are the frequencies of an undamped steel cylindrical shell ($\ell=900$ cm, $2h_1=0.33$ cm, $a=25.4$ cm, $E=2.1\times10^6$ kg/cm^2, $\rho=8.01\times10^{-6}$ kg sec^2/cm^4) with the pressurized water enclosed ($c=15.24\times10^4$ cm/sec, $\rho_f=1.0\times10^{-6}$ kg sec^2/cm^4, $p=27$ kg/cm^2). The experimental and theoretical solutions determined by Shiraki et al.[12] and by Eq. (25) are tabulated. For the modes considered, it is shown clearly that all of the analytical and experimental results are in excellent correlation. The significant difference between these theoretical solutions is that the enclosed fluid is considered compressible in Eq. (25) whereas Shiraki et al. consider it incompressible. It is well known that the compressibility of a fluid may be neglected only if the frequency is low compared to the quantity λ. As shown in the table, the present solutions are getting better and better as the frequencies increase. This results from the consideration of the compressibility of the enclosed fluid. Other differences are that the present

Table 1 Comparison between frequencies of an undamped shell filled with pressurized water—analytical results vs experimental data

	Frequencies, Hz		
		Analytical solutions	
	Experimental data	Present solutions	Shiraki et al.
$n=2, m=1$	72.2	72.8	72.0
$n=2, m=2$	77.0	73.9	72.5
$n=2, m=3$	80.6	77.2	75.5
$n=2, m=4$	81.7	84.4	83.0
$n=2, m=5$	105.5	97.3	96.7
$n=2, m=6$	117.2	115.8	118.0
$n=3, m=2$	148.2	146.1	144.0
$n=3, m=6$	155.0	155.7	152.0
$n=3, m=7$	162.0	162.4	158.9

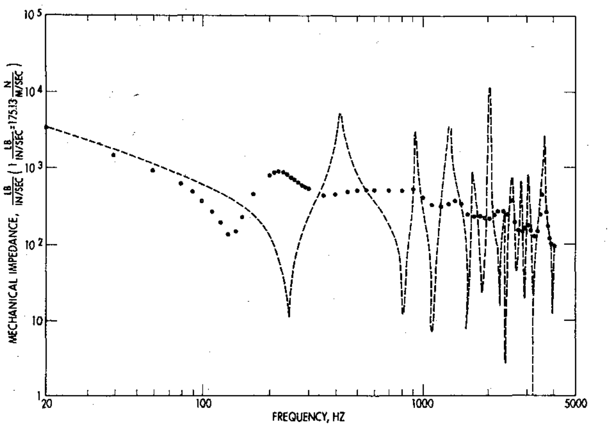

Fig. 4 Driving point mechanical impedances of a damped and an undamped shell (no water is enclosed).

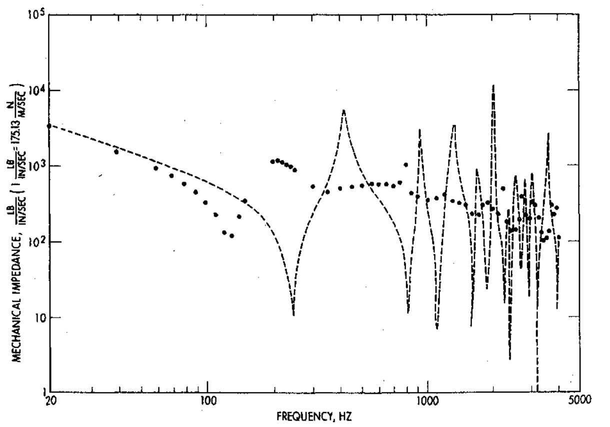

Fig. 5 Driving point mechanical impedances of a damped shell with pressurized water enclosed.

frequency equation is derived from the Flügge's equation whereas Shiraki's[12] frequency equation is obtained by an energy approach and is reduced to a rather simple expression by using the assumption of zero hoop and shear strain in addition to ones of thin shell theory.

IV. Numerical Solutions and Discussion

The analytical procedure outlined herein is used to calculate the radial driving point mechanical impedance for a damped system of interest. The system is a pressurized water-filled cylindrical steel elastic shell having 12 identical mass segments adhered to it by a viscoelastic material. The mass segments are made of a material whose density is assumed 20 times heavier than that of steel, and are assumed uniformly distributed around the circumference of the center section of the shell. The density of the mass segment is so chosen because we intend in the future to compare on the same weight (or mass) basis this numerical solution to those of yet another damped cylindrical system of interest in which longitudinal beams (20 times longer than the axial length of the mass segments), instead of the mass segments, are adhered to it by a viscoelastic material. The viscoelastic layer used here in the example is an acrylic base material with a complex shear modulus at 24°C that can be calculated for the frequency range of interest by

$$G^* = 6895(1+i\beta)\exp[0.5\ln(\Omega/2\pi)+3.022] \text{ pascal} \tag{26a}$$

$$\beta = 1.46 \tag{26b}$$

The geometrical dimensions of the system are $\ell = 152.4$ cm, $2h_l = 1.27$ cm, $a = 10.3$ cm, $2h_2 = 8.89\times 10^{-2}$ cm, $b_i = 5.08$ cm, $d_i = 7.62$ cm, $2h_i = 1.27$ cm. The end conditions of the shell are assumed to be simply supported. In the example problem of interest, the source of excitation is a concentrated vibratory radial force with circular frequency Ω, located on the middle surface of the shell midway between two mass segments and half the distance along the length, i.e., $\theta_c = 0$ and $x_c = \ell/2$. Because of the uniformity of the attachment of the mass segments, the symmetric property with respect to $\theta = 0$, does exist. The theoretical solutions obtained are the summation of the first 10 circumferential modes and the first 11 contributing longitudinal half-wave numbers. Equation (16) is evaluated by the inversion of the matrix, and the inversion is computed by the Gauss-Jordan elimination method.

In Fig. 4, the driving point mechanical impedances for the given damped system (circles) are presented. In this system, no water is filled in the shell. For comparison purposes, the corresponding solutions of the undamped system, also without the presence of water (broken line), i.e., with the viscoelastic layer and mass segments omitted, also are given in this figure. In the frequency region of interest and for the specific configurations under consideration, the responses for the damped and the undamped systems are obviously different. In the lower frequency region, both systems follow the same stiffness line in the impedance plot. This implies that the addition of the heavy mass segments does not effect the stiffness of the system. However, the lowest fundamental frequency of the damped system is reduced to about half the value of that of the undamped system because of approximately 94% of the mass added to the system. In the frequency region beyond this fundamental frequency the responses of the damped system are damped considerably as compared with those of the undamped system.

In calculating the responses and the frequencies of the undamped system, the procedure is standard and straightforward. The importance of the investigation of this special case is that the vibration of the undamped system may be used to serve as a basis to evaluate the damping mechanism and the effectiveness of the mass segments attached damping system. To demonstrate and to identify the resonance frequencies of the impedance plot, the frequencies in the range of interest calculated for this particular undamped system are listed in Table 2.

For a damped shell filled with pressurized water, the driving point mechanical impedance is presented in Fig. 5. Other than the enclosed pressurized water, the geometry and the material properties of the system are the same as those given in Fig. 4. The water pressure is assumed to be 28.2 kg/cm^2. The responses of the undamped shell without the presence of water also are given for references. Comparing to Fig. 4, the responses of this damped shell system with and without the water is slightly different except that the fundamental frequency for the pressurized water-filled shell is slightly lower. It is believed that this is not significant because the attached mass segments have dominant effects in the response of this particular case.

To demonstrate the effects of the presence of the pressurized water, the responses of the undamped shell with (dot-broken line) and without (broken line) water are given in Fig. 6. The undamped system is the same as that presented before in Fig. 4, and the water pressure is assumed to be 28.2 kg/cm^2. It can be seen that the presence of the pressurized water reduces the frequencies significantly. The driving point mechanical impedances for the pressurized water-filled shell are given only up to 2 KHz. This is because the lines in the

Table 2 Frequencies of an undamped shell without water filled

	Frequencies, Hz				
n/m	1	3	5	7	9
1	241	1598	3187	4576	5704
2	809	1097	1884	2890	3919
3	2263	2374	2673	3200	3912

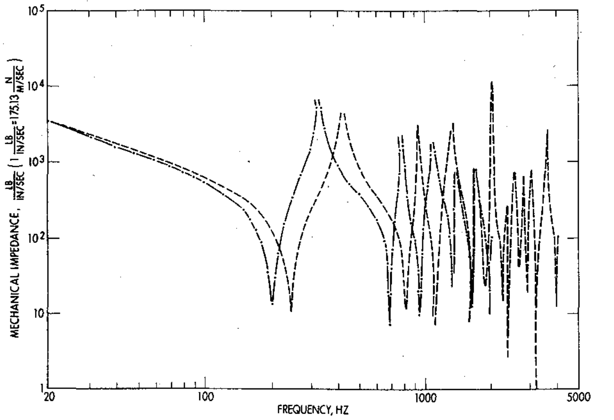

Fig. 6 Comparison of responses of an undamped shell with and without pressurized water.

Table 3 Comparison between frequencies of an undamped shell with and without pressurized water[a]

	Frequencies, Hz				
n/m	1	3	5	7	9
1	197 (241)	1315 (1598)	2548 (3187)	3534 (4596)	
2	688 (809)	933 (1097)	1604 (1884)	2463 (2890)	3338 (3919)
3	1977 (2263)	2078 (2374)	2346 (2673)	2815 (3200)	3448 (3912)

[a] Numbers in parentheses are the frequencies of the undamped shell without pressurized water.

higher-frequency region are too crowded to be seen distinctively. For clarity and for comparison purposes, the frequencies for these two systems are listed in Table 3.

V. Conclusions

In summary, this paper has presented an analysis for the forced vibratory responses of a pressurized liquid-filled cylindrical shell having a number of mass segments adhered to it by a viscoelastic material. The mass segments are distributed discretely around the outer circumference at an arbitrary section of the shell. The end conditions of the shell are assumed simply supported. The liquid is considered as a compressible and inviscid fluid. The viscoelastic material is assumed incompressible. Since the formulation is presented in a very general fashion, the attachments may be arranged arbitrarily. The driving point mechanical impedances are given for a location midway between two mass segments and half the distance along the length for a given damped system with or without the pressurized water. These solutions are compared and discussed, respectively, with those of an undamped shell. For the particular configuration given, the damping effects are significant. The responses of a discontinuously constrained damped ring configuration without liquid enclosed, and the frequencies of an undamped shell filled with pressurized water, which are the special cases derived from the analysis presented, respectively, compare very well with the available experimental data. For the system of interest, it is obvious that the vibrational behavior of such a damped shell is complicated by the involvement of many parameters. It depends upon the geometries of the shell element, the attached mass segments, the thickness of the viscoelastic layer, the pressure of the enclosed fluid, and the properties of elastic and viscoelastic materials. General conclusions regarding the best arrangement to be used in a specific application can not be drawn easily. For the optimization of design for any particular specification, a complete parametric study is required.

Acknowledgment

All opinions or assertions made in this paper are those of the author and are not to be construed as official or necessarily reflecting the views of the Navy or the naval service at large.

References

[1] Kerwin, E. M., Jr., "Damping of Flexural Waves by a Constrained Viscoelastic Layer," *Journal of the Acoustical Society of America*, Vol. 31, July 1959, pp. 952-962.

[2] DiTaranto, R. A., "Theory of Vibratory Bending for Elastic and Viscoelastic Layered Finite-Length Beams," *Journal of Applied Mechanics*, Vol. 32, Dec. 1965, pp. 881-886.

[3] Mead, D. J. and Markus, S., "The Forced Vibration of a Three-Layer Damped Sandwich Beam with Arbitrary Boundary Conditions," *Journal of Sound and Vibration*, Vol. 10, No. 2, 1969, pp. 163-175.

[4] Agbasiere, J. A. and Grootenhuis, P., "Flexural Vibration of Symmetrical Multi-Layer Beams with Viscoelastic Damping," *Journal of Mechanical Engineering Science*, Vol. 10, No. 3, 1968, pp. 269-281.

[5] Oberst, H., "Reduction of Noise by the Use of Damping Materials," *Royal Society of London, Philosophical Transactions*, Ser. A, Vol. 263, Dec. 1968, pp. 441-453.

[6] Ruzicka, J. E., "Damping Structural Resonances Using Viscoelastic Shear-Damping Mechanisms, Part I—Design Configurations," *Journal of Engineering for Industry*, Vol. 83, Nov. 1961, pp. 403-413.

[7] Ruzicka, J. E., "Damping Structural Resonances Using Viscoelastic Shear-Damping Mechanisms, Part II—Experimental Results," *Journal of Enginering for Industry*, Vol. 83, Nov. 1961, pp. 414-424.

[8] Ungar, E. E. and Kerwin, E. M., Jr., "Damping of Composite Structures by Viscoelastic Interlayers," *Journal of the Acoustical Society of America*, Vol. 32, July 1960, p. 912(A).

[9] DiTaranto, R. A., Lu, Y. P., and Douglas, B. E., "Forced Response of a Discontinuously Constrained Damped Ring," *Journal of the Acoustical Society of America*, Vol. 54, July 1973, pp. 74-79.

[10] Lu, Y. P., "An Analytical Formulation of the Forced Responses of Damped Rings," *Journal of Sound and Vibration*, Vol. 48, No. 1, 1976, pp. 27-33.

[11] Flügge, W., *Stresses in Shells*, Springer-Verlag, New York, 1966.

[12] Shiraki, K., Honma, T., and Nagata, O., "The Penstock Vibration Characteristics—On the Vibrations of Simply Supported and Ring-Stiffened Cylindrical Shells Filled with Pressurized Water," ASME Paper 75-DET-114, Sept. 1975.

[13] Cramer, W. S., "Propagation of Stress Waves in Rubber Rods," *Journal of Polymer Science*, Vol. XXVI, 1957, pp. 57-65.

[14] Nashif, A. D., "New Method for Determining Damping Properties of Viscoelastic Materials," *Shock and Vibration Bulletin*, Vol. 36, Pt. 4, Feb. 1967, pp. 37-47.

[15] Jones, D. I. G., "Temperature-Frequency Dependence of Dynamic Properties of Damping Materials," *Journal of Sound and Vibration*, Vol. 33, No. 4, 1974, pp. 451-470.

[16] Roscoe, A. J., III, Thomas, E. V., and Blasingame, W., "Measurement of Complex Shear Modulus of Viscoelastic Materials by Mechanical Impedance Methods," *Shock and Vibration Bulletin*, Vol. 35, Pt. 7, April 1966, pp. 267-274.